

# Thermal conductive properties of a semiconductor laser on a polymer interposer

Takeru Amano<sup>1,2</sup>, Shigenari Ukita<sup>1,2</sup>, Laina Ma<sup>1,2</sup>, Masahiro Aoyagi<sup>1,2</sup> and Kazuhiro Komori<sup>1,2</sup>

<sup>1</sup> Photonics Electronics Technology Research Association (PETRA),  
1-20-10 Sekiguchi, Bunkyo-ku, Tokyo 112-0014, Japan

Phone: +81-29-861-9237 E-mail: takeru-amano@aist.go.jp

<sup>2</sup> National Institute of Advanced Industrial Science and Technology (AIST),  
Umezono, Tsukuba, Ibaraki 305-8568, Japan

## 1. Introduction

The demand for high-speed and high-density interconnection in high-performance computing systems and high-end servers is growing quickly, as their performance continues to improve with the evolution of complementary metal-oxide-semiconductor technologies. However, conventional electrical interconnections are approaching critical limits of transmission bandwidth and physical space. Optical interconnection technologies can solve these problems. Active optical cable (AOC) has recently been used for rack-to-rack interconnection. On-board optical interconnection is required at higher bit rates because there are problems with electrical signal integrity. Optical modules can be aligned near large scale integration (LSI) systems to reduce signal distortion in electric transmission lines. Recently, several studies have been conducted concerning on-board optical interconnection using waveguides embedded in printed circuit boards (PCBs) [1, 2]. However, thermal issues are caused by the optical transmitter in the case of AOC and PCBs. In this work, we calculated the thermal conductive properties and rising temperature speed of a semiconductor laser. Moreover, we measured the heat distribution and rising temperature speed of a quantum dot (QD) laser on a polymer.

## 2. Calculation of thermal conductive properties

We calculated heat conduction properties using the three-dimensional finite element method (FEM) for the laser on a polymer interposer. The laser structure consists of a GaAs substrate, a lower AlGaAs cladding layer, a GaAs active layer, and an upper AlGaAs cladding layer. The laser integrates with the polymer interposer using Au film. Table 1 lists the parameters of the laser on the polymer interposer. The parameters of the setup were taken assuming a cooling location at the bottom of the interposer and a temperature of 20 °C.

Table 1 Parameters of simulation model

Part	Material	Scale (width, length, thickness) [ $\mu\text{m}$ ]	Specific heat [ $\text{Jkg}^{-1}\text{K}^{-1}$ ]	Thermal conductivity [ $\text{Wm}^{-1}\text{K}^{-1}$ ]
Interposer	PMMA	2000, 1000, 150	1400	0.16
Interface	Au film	2000, 1000, 0~0.5	130	295
Laser_active	GaAs	1.5, 1000, 1	325	48
Laser_clad	AlGaAs	200, 1000, 2	547	12
Laser_sub	GaAs	200, 1000, 150	325	48

The Au film interface between the polymer interposer and laser is important for heat distribution. We calculated the laser temperature on the polymer for several thicknesses of the Au film. The heating location was assumed to be at the laser active region, and the energy was assumed to be 10 mW. The temperature rose to 55 °C in the case without the Au film. When the temperature rose to 27 °C on the polymer interposer, the heat radiation effect was almost saturated in the case of the Au film with a thickness of 500 nm.

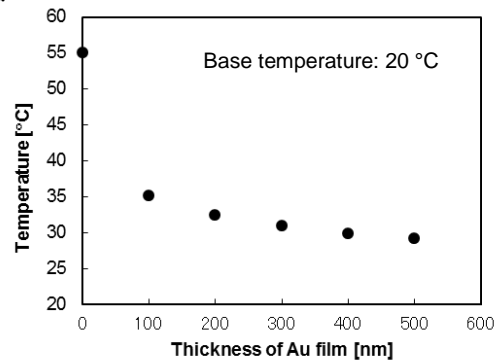


Fig.1 Rising temperature characteristics

When a laser is used, it is expected that its operation becomes unstable until the temperature is stable. Therefore, the rise time of the heat generated by the laser was estimated. Figure 2 shows the calculated results of the temperature rising speed at a heat generation of 50 mW. According to calculated results, 98% of the temperature increase occurs 0.5 s after the laser starts functioning.

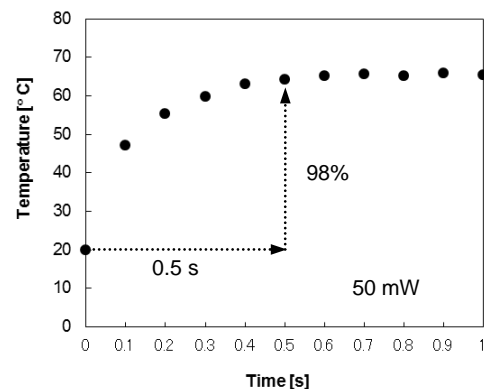


Fig. 2 Calculated results of temperature rising speed

### 3. Measurement of heat distribution

We placed a QD laser on a polymer interposer using solder with a low melting point and evaluated the thermal properties. We could realize a 1.3- $\mu\text{m}$  QD with a high density of  $8.0 \times 10^{10} \text{ cm}^{-2}$  generated by an  $\text{As}_2$  source [3]. The laser wafer structure was the same as that of the simulated one. The QD laser structure was high mesa stripe, with a height and width of 2.6  $\mu\text{m}$  and 2.8  $\mu\text{m}$ , respectively. After the etching process, the laser structure was fabricated by a standard process. The facets were as-cleaved, and no coating was applied [4]. Au film with 500 nm thickness was fabricated on a polymer substrate. We achieved a low threshold current operation of 15 mA at 1.31  $\mu\text{m}$  in the QD laser with a cleaved facet. Figure 3 shows the I-V and I-L characteristics before and after QD laser bonding on the polymer, respectively. The QD laser was measured at room temperature under pulse operation. The electrical resistance of the QD laser on the polymer increased from 11.6  $\Omega$  to 14.6  $\Omega$ . Also, the laser threshold increased from 15 mA to 16 mA. The calculated result of the rising temperature at an injection current of 30 mA was a 4  $^\circ\text{C}$  temperature increase in the case of 3- $\Omega$  bonding resistances. From these results, temperature characteristic  $T_0$  of the threshold current was determined as 62 K at the QD laser on the polymer. By optimizing the QD laser on the polymer using a solder with a low melting point, we could suppress the degradation of the laser characteristics for the contact resistance.

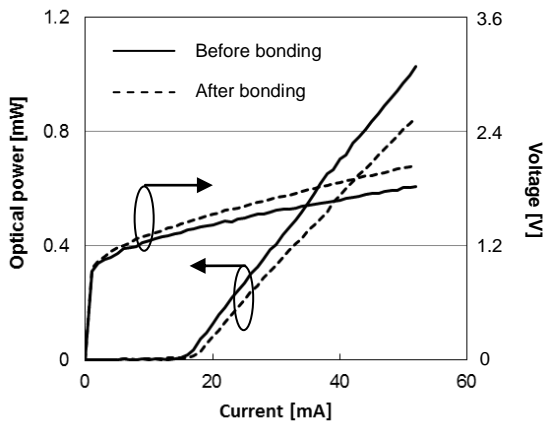


Fig. 3 I-V and I-L characteristics.

We measured the speed of the temperature change of a QD laser on a polymer using an infrared radiation thermometer at 20  $^\circ\text{C}$ . Figure 4 shows the rising temperature speeds at injection powers of 20 mW and 50 mW. The final maximum temperatures at 20 mW and 50 mW were 37  $^\circ\text{C}$  and 63  $^\circ\text{C}$ , respectively. The calculated results of the final maximum temperatures at 20 mW and 50 mW were 38  $^\circ\text{C}$  and 66  $^\circ\text{C}$ , respectively. The calculated temperatures almost matched the experimental results. In addition, the experimental rising speed and a calculated rising speed at 20 mW and 50 mW occurred at almost the same rate of 0.5 s.

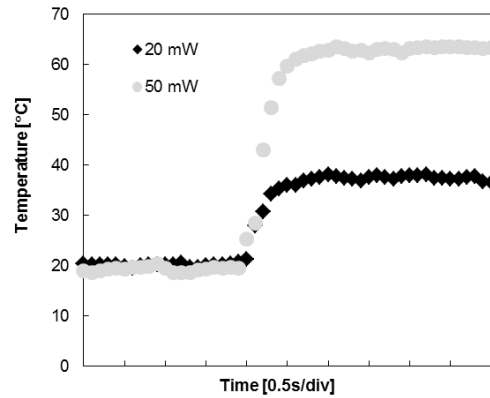


Fig. 4 Rising temperature speeds at injection powers of 20 mW and 50 mW.

### 4. Conclusions and discussion

In this work, we calculated the thermal conductive properties and rising temperature speed of a laser on a polymer board. The temperature rose to 55  $^\circ\text{C}$  in the case without a Au film at 10 mW. The temperature rose to 27  $^\circ\text{C}$  on the polymer interposer and the heat radiation effect was almost saturated in the case where the Au film had a thickness of 500 nm at 10 mW. Further, we measured the thermal conductive properties and rising temperature speed of a QD laser on a polymer board. The calculated and experimental data were almost identical. Additionally, we estimated the operating restrictions of a laser in a server computer. The background temperature of a server computer is approximately 60  $^\circ\text{C}$ . The operating temperature of a conventional laser is below 85  $^\circ\text{C}$ . The operating heat limit in the case of a laser without a Au film on a polymer board is 8 mW. Moreover, the operating heat limits in the case of a 100-nm Au film and a 500-nm Au film are 17 mW and 28 mW, respectively. If the wall plug efficiency of the laser is 20%, the laser output power is 2 mW, 4 mW, and 7 mW for a laser on a polymer without a Au film, with a 100-nm Au film, and with a 500-nm Au film, respectively. These results indicate that we need to realize a high efficiency laser source to achieve high transmission speeds in the future. In addition, we need to develop a light source that functions sufficiently fast producing higher temperatures operation than 85  $^\circ\text{C}$ .

### Acknowledgements

A part of this work was supported by the “Next-generation High-efficiency Network Device Project,” contracted by PETRA with the New Energy and Industrial Technology Development Organization (NEDO).

### References

- [1] J. A. Kash et al., Proc. OFC’10, OtuH3 (2010).
- [2] Y. Matsuoka et al., Proc. OFC’10, JThA58 (2010).
- [3] T. Amano et al., Jpn. J. Appl. Phys., 44, L432 (2005)
- [4] T. Amano et al., Proc. ISLC’08, P19 (2008).